

Collective character of spin excitations in a system of Mn^{2+} spins coupled to a two-dimensional electron gas

F.J. Teran, M. Potemski, D.K. Maude, D. Plantier, A.K. Hassan, and A. Sachrajda*
*Grenoble High Magnetic Field Laboratory, Max Planck Institut für Festkörperforschung
and Centre National de la Recherche Scientifique, BP 166, 38042 Grenoble Cedex 9, France.*

Z. Wilamowski, J. Jaroszynski, T. Wojtowicz, and G. Karczewski
Institute of Physics, Polish Academy of Sciences, 02668 Warsaw, Poland
(Dated: July 1, 2020)

We have studied the low energy spin excitations in n-type CdMnTe based dilute magnetic semiconductor quantum wells. For magnetic fields for which the energies for the excitation of free carriers and Mn spins are almost identical an anomalously large Knight shift is observed. Our findings suggest the existence of a magnetic field induced ferromagnetic order in these structures, which is in agreement with recent theoretical predictions [J. König and A. H. MacDonald, submitted Phys. Rev. Lett. (2002)].

PACS numbers: 73.43.-f, 75.50.P, 72.20

Although the existence of a ferromagnetic phase in diluted magnetic semiconductors (DMS) is experimentally well established[1, 2, 3, 4], the physical origin of this phenomenon is far from being well understood[5, 6, 7]. The RKKY approach [8], which successfully explains the ferromagnetism observed in magnetic metals, cannot easily be applied to the case of magnetic semiconductors which are typically composed of a dilute subsystem of localized magnetic spins and an even more dilute gas of free carriers. On the other hand, the early Zener model[9] of ferromagnetism driven by the exchange interaction between free carriers and localized magnetic moments provides a rough estimate of the observed critical ferromagnetic temperatures in DMS materials[5]. The Zener model nevertheless neglects important effects related to the character of the ferromagnetic order in these systems, possibly mediated by the itinerant nature of the free carriers spins[7]. This suggests that diluted magnetic semiconductors show a new class of ferromagnetism, which however, remains to be experimentally verified.

In this letter, we report on the investigations of spin excitations in a model DMS structure, namely very diluted Mn^{2+} ions coupled to an electron gas both of which are confined in a CdMnTe quantum well structure. Our key experimental results rely on an accurate and local probing of Mn^{2+} spin excitations using the electron paramagnetic resonance (EPR) technique. At low magnetic fields ($B < 4T$) and sufficiently high temperatures ($T \sim 4.2K$), the investigated structure show all the attributes of a system composed of two paramagnetic subsystems: localized Mn^{2+} ions and an electron gas, coupled via the $s-d$ exchange interaction. The main experimental finding reported here is the change in the line-shape and the giant shift of the Mn^{2+} resonance observed under specific conditions when the spin polarization of free carriers is induced by the application of the high magnetic field and when at the same time the energies of the mean field spin

excitations of electron's and Mn^{2+} spins are comparable. This finding can be considered as a positive test for the recent theory of ferromagnetism in DMS materials[7]. The observed changes in the spin resonance spectrum indicate the formation of two macroscopic moments characteristic for each spin subsystem, which are efficiently coupled via their transverse components. Although the expected zero-field ferromagnetic critical temperature for the investigated n-type structures is expected to be very low ($\lesssim 5mK$) [10], our data suggest the appearance of ferromagnetic order in these systems when the spin polarization is forced by the application of a magnetic field.

The two samples A and B used for investigations were 10nm-thick CdMnTe/CdMgTe single quantum well structures with a modulation doping on one side of the quantum well (QW). Both samples have been characterized by conventional magneto-luminescence measurements whereas sample B has also been intensively studied with magneto-transport and cyclotron resonance absorption measurements [11]. In sample A, the estimated electron sheet density is $n_e \simeq 1 \times 10^{11} \text{cm}^{-2}$ (corresponding 3D concentration $n_e^{3D} \simeq 1 \times 10^{17} \text{cm}^{-3}$), and an effective Mn^{2+} concentration in the QW $x_{eff} \simeq 0.2\%$ ($n_{Mn}^{3D} \simeq 3 \times 10^{19} \text{cm}^{-3}$). The parameters of sample B are more precisely determined: $n_e = 5.95 \times 10^{11} \text{cm}^{-2}$, ($n_e^{3D} \simeq 6 \times 10^{17} \text{cm}^{-3}$), mobility $\mu = 60000 \text{cm}^2/\text{Vs}$ and $x_{eff} = 0.3\%$ ($n_{Mn}^{3D} \simeq 4.4 \times 10^{19} \text{cm}^{-3}$).

The spin excitations have been probed using Raman scattering and resistively detected multi-frequency EPR. Raman scattering allows to probe the spin flip transitions of both band electrons and Mn^{2+} ions but can only be easily applied for samples with low electron concentrations, which show sharp (exciton like) absorption lines and therefore a large resonant enhancement of the scattering signal. Traditional EPR techniques give a higher resolution, but are difficult to apply in our case due to the small number of spins. Here we locally probe the

Mn²⁺ EPR in CdMnTe quantum wells via detecting the microwave induced changes in the longitudinal resistance using microwave sources (operating at 95 GHz and 230 GHz (Gunn diodes) and in the range of 64-95 GHz (cavitrans)).

In a first approach, we consider the system to be composed of two paramagnetic subsystems: two-dimensional conduction electrons with extended wave functions and localized $3d^5$ states of Mn²⁺ ions, which interact via the $s-d$ exchange interaction. Reasoning in terms of the conventional mean field approximation, we expect the energies of spin excitations for electrons, E_e^S , and Mn²⁺ ions, E_{Mn}^S to be: $E_e^S = E_e^Z + \Delta_E$ and $E_{Mn}^S = E_{Mn}^Z + K_E$, where, correspondingly for electrons and Mn²⁺ ions, E_e^Z and E_{Mn}^Z are the energies in the absence of the $s-d$ exchange interaction, whereas Δ_E and K_E denote the mean field exchange terms. We consider only the relevant spin excitations with $|\Delta m_S| = 1$, (m_S is the quantum number associated with the projection of the spin along the external magnetic field direction) and in a first approximation assume that E_e^Z and E_{Mn}^Z are given by the usual Zeeman terms: $E_e^Z = g_e \mu_B B$ and $E_{Mn}^Z = g_{Mn} \mu_B B$ (throughout this paper we take $g_e = -1.64$ and $g_{Mn} = 2.007$ for the electronic and Mn²⁺ g-factors, respectively [12, 13]). Including the mean field $s-d$ exchange, the characteristic spin excitations of our system can be expressed as follows:

$$E_e^S = E_e^Z + \Delta_E = g_e \mu_B B + J_{sd} n_{Mn}^{3D} \frac{5}{2} \sigma_{Mn}^z \quad (1)$$

$$E_{Mn}^S = E_{Mn}^Z + K_E = g_{Mn} \mu_B B + J_{sd} n_e^{3D} \frac{1}{2} \sigma_e^z \quad (2)$$

Here, $\frac{1}{2} \sigma_e^z$ and $\frac{5}{2} \sigma_{Mn}^z$ denote mean values of the S_z spin components, correspondingly, for electrons (with spin $S=1/2$) and Mn²⁺ ions (with spin $S=5/2$), and J_{sd} is the exchange constant. σ_{Mn}^z and σ_e^z should be identified with the normalized (to unity) spin polarization of Mn²⁺ ions and electrons, respectively. Rewriting the above equations in the following form:

$$E_e^S = g_e \mu_B \left(B + \frac{\Delta_E}{g_e \mu_B} \right) = g_e \mu_B (B + \Delta_B) \quad (3)$$

$$E_{Mn}^S = g_{Mn} \mu_B \left(B + \frac{K_E}{g_{Mn} \mu_B} \right) = g_{Mn} \mu_B (B + K_B) \quad (4)$$

there is an evident analogy between physics of DMS materials and that of nuclear spins in metals coupled to the electrons spins via the hyperfine interaction. Whereas the Overhauser shift, Δ_B (energy, Δ_E) is expected to be significant in our structures ($\Delta_E^{\max} = J_{sd} n_{Mn}^{3D} \frac{5}{2} \sim 1.5 meV$), the Knight shift K_B (energy, K_E) is much more subtle: $K_E^{\max} / \Delta_E^{\max} = n_e^{3D} / 5 n_{Mn}^{3D}$, so that $K_E^{\max} = J_{sd} n_e^{3D} \frac{1}{2} \sim 1 - 4 \mu eV$.

An overview of the relevant spin excitations for the investigated system can be obtained from Raman scattering spectra. The measured energies of the excitations, which can be easily identified with the spin-flip

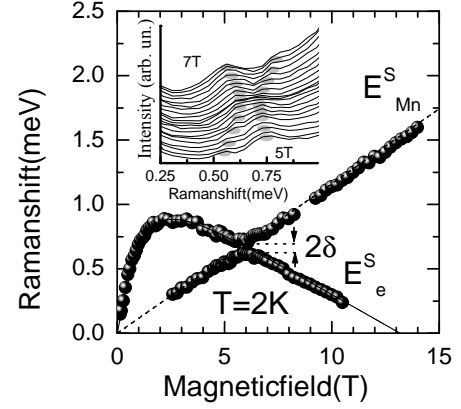


FIG. 1: Raman shift for the spin-flip transitions for electrons and Mn²⁺ ions for sample A. The expected behavior for non interacting subsystems calculated as described in the text is indicated by the solid and dashed lines. The inset shows the Raman spectra (every 0.1T) in the region of the avoided crossing. The shaded regions are a guide to the eye.

transitions for electrons and Mn²⁺ ions are shown in Fig.1. The solid line represents the E_e^S versus B dependence according to Eq(1) assuming that the spin polarization of Mn²⁺ is given by the modified Brillouin function: $\sigma_{Mn}^z = B_{5/2}(g_{Mn} \mu_B B / k(T + T_0))$, with two adjustable parameters: the saturated value of the exchange term $\Delta_E^{\max} = J_{sd} n_{Mn}^{3D} \frac{5}{2} = 1.25 meV$ and $T_0 = 0.12 K$ which phenomenologically accounts for the small antiferromagnetic correction for the Mn²⁺ ensemble. Note, that the signs of the electron g-factor and the exchange constant in CdMnTe are such that the effective electron spin splitting results from the competition between the intrinsic Zeeman term and the $s-d$ exchange contribution (we use the convention that $E_e^Z < 0$ and $\Delta_E > 0$). The dashed, line in Fig.1 is the predicted linear variation of the Mn²⁺ spin excitations when neglecting the small Knight shift and possible subtle corrections to the Mn²⁺ spin Hamiltonian related to hyperfine interaction and/or crystal field effects which are in any case beyond the resolution of the Raman scattering data. This simple model satisfactorily reproduces the observed spin excitation energies except in the region around $\sim 5 T$ where $E_e^S \sim E_{Mn}^S$ in sample A. A clear indication of the avoided crossing of electron and Mn²⁺ spin excitation with the characteristic repulsion energy $2\delta \approx 0.08 meV$ is observed (see inset to Fig.1). This is our key experimental observation, which will be further elucidated using the more precise EPR spectroscopic tool.

Sample B, chosen for the resistively detected EPR measurements, has been prepared in the form of a 0.5 x 1 mm Hall bar. As illustrated in Fig.2(a), it shows typical magneto-transport properties for a 2-DEG. Using the available microwave sources, the resonant change in the longitudinal resistance induced by microwave illumina-

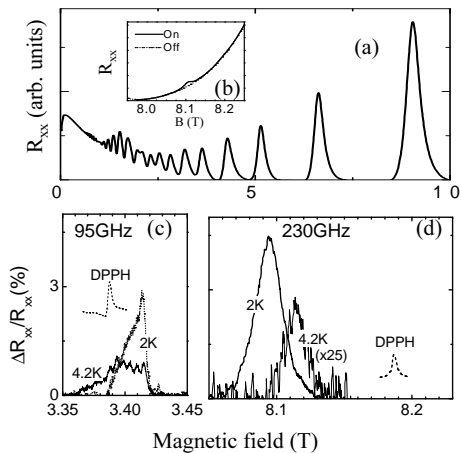


FIG. 2: (a) Longitudinal resistance R_{xx} as a function of magnetic field. (b) R_{xx} with and without 230 GHz microwave illumination. (c) and (d) Typical resistively detected EPR spectra. The EPR spectra of the DPPH g-factor marker is shown for comparison.

tion and identified with the Mn^{2+} EPR signal, has been measured at magnetic fields $B \sim 2.4, 2.7, 3.5$ and 8.1 T (correspondingly, in the vicinity of filling factors $\nu=10, 9, 7$ and 3). The measurements around $B \sim 8.1$ T correspond to the case when the energy of the spin excitations of the E_e^S , and E_{Mn}^S subsystems are expected to be almost identical in sample B. An example of the measured resonant increase of the R_{xx} around 8.1 T ($\nu \sim 3$) is illustrated in Fig.2(b), where an expanded view of (R_{xx}) is shown with and without microwave illumination at 230 GHz. In order to calibrate exactly the magnetic field value, a small amount of a g-factor marker diphenylpicryl-hydrazyl (DPPH) with $g=2.0036$ is placed close to the sample and its EPR spectrum is simultaneously measured using carbon bolometer mounted below the sample. Typical EPR spectra obtained by subtracting the resistance measured with and without microwave illumination (ΔR_{xx}) when using 95 GHz and 230 GHz microwave sources are shown in Fig.2(c) and (d) for two different temperatures.

The spectrum measured at 95 GHz and 4.2K can be recognized as the typical signal of paramagnetic Mn^{2+} ions. It shows six relatively well pronounced components which result from the hyperfine interaction between the spin of the Mn $3d^5$ electrons and the Mn nuclear spin ($I=5/2$). The estimated hyperfine splitting (constant) is 52 G ($A_{Mn} = 49 \times 10^{-4} \text{cm}^{-1}$). The smaller signal on the low field side of the main spectrum (which characteristically vanishes at lower temperatures) is due to the fine splitting which results from crystal field effects related to the strain present in the quantum well. The estimated value of the fine constant is $D = 47 \times 10^{-4} \text{cm}^{-1}$. The amplitude and shape of the resonance measured at low magnetic fields depends strongly on temperature in the

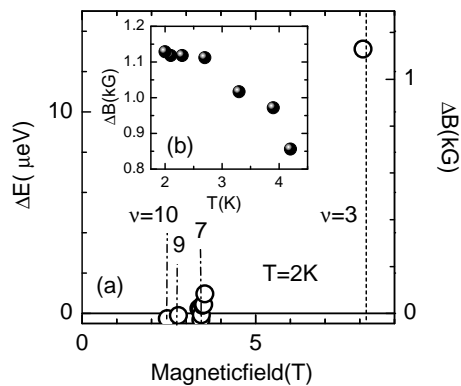


FIG. 3: (a) Measured shift of the Mn^{2+} EPR line from the expected behavior. (b) Temperature dependence of the large shift observed close to filling factor $\nu = 3$.

range between 4.2 and 2 K (see Fig.2(c)). At $T=2$ K, as expected only the main fine component is observed but surprisingly enough the amplitudes of the hyperfine satellites are significantly modified and/or the spectrum shape is significantly changed. This unusual spectral shape at $T = 2$ K either results from the effect of dynamical nuclear polarization or indicates that the measured resonance can no longer be attributed to paramagnetic Mn^{2+} centers which then can be considered a first signature of a change of the magnetic phase of the Mn^{2+} ensemble at low temperatures even at low magnetic fields.

The EPR spectra measured at 230 GHz around $B=8$ T are distinctly different (Fig.2(d)). No trace of hyperfine splitting is found. Instead the spectrum represents a symmetric, relatively narrow single line. What is even more significant is that the position of this line is shifted far from the value expected from a simple linear extrapolation. This can clearly be seen in the raw data from the respective positions of Mn^{2+} and DPPH resonances measured at 95 and 230 GHz shown in Figs.2 (c) and (d), and is more clearly illustrated in Fig.3, where the difference between the measured resonance energies (magnetic field position) and those given by $E_{Mn}^S = g_{Mn} \mu_B B - 4D$ as expected for the low temperature paramagnetic Mn^{2+} resonance are plotted for the data obtained at 2K at different magnetic fields. While the above formula correctly reproduces the resonance position at low fields, a very large shift of the resonance (~ 1100 G) towards lower fields can be deduced for the 230 GHz spectra. As shown in Fig.2 (d) and Fig.3, the 230 GHz-resonance position is remarkably sensitive to temperature. A shift of ~ 300 G is observed when the temperature is increased from 2 K to 4.2 K. At first sight one might think that the observed change in the resonance position can be simply related to a conventional Knight shift. However, the saturated value of the Overhauser shift in this sample has been precisely determined from the low field transport measurements ($\Delta E^{\text{max}} = 1.65 \text{meV}$)[11]. Thus the expected amplitudes

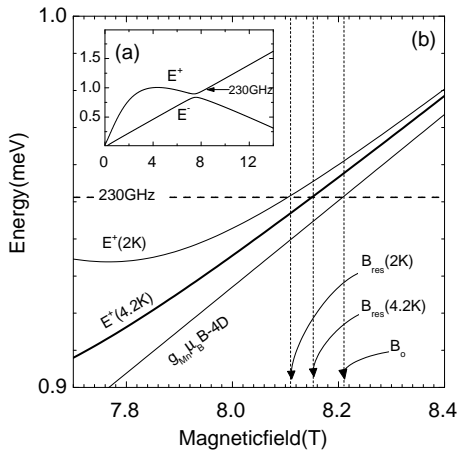


FIG. 4: (a) Predicted spin excitations using the phenomenological perturbation model as described in the text. (b) Expanded view of the avoided crossing region.

of Knight shift are $K_E = \Delta_E^{\max}(n_e^{3D}/5n_{Mn}^{3D})\sigma_e^z = 4.5\sigma_e^z$ [μeV], where the maximum electron spin polarization can be estimated from Landau level filling factors $\sigma_e^z \leq 1/\nu$ (for odd filling factors). Therefore, around $B=8$ T (where $\nu \sim 3$): $K_E \leq 1.5\mu\text{eV}$ (or $K_B \leq 130\text{G}$) and for the case of experiments at low magnetic fields (where $\nu \geq 7$): $K_E \leq 0.7\mu\text{eV}$ (or $K_B \leq 40\text{G}$). As can be seen in Fig.3, in the range of low magnetic fields the measured resonance positions are consistent with the expected Knight shift but this conventional effect is clearly unable to account for either the observed position of the 230GHz resonance or for its temperature dependence.

Phenomenologically the position of the 230 GHz resonance can be explained by taking into account the effect of the interaction between the mean field modified E_e^S and E_{Mn}^S spin excitations of the 2D electron and the Mn^{2+} ensembles, respectively. This manifest itself as the avoided crossing of the corresponding excitation energies as already indicated by our Raman scattering data for sample A. To simulate such an effect, we introduce the coupling between E_e^S and E_{Mn}^S excitations using a simple perturbation approach and obtain: $E^\pm = \frac{1}{2}(E_e^S + E_{Mn}^S) \pm \frac{1}{2}\sqrt{(E_e^S - E_{Mn}^S)^2 + 4\delta^2}$ for the new coupled modes (2δ is the characteristic repulsion energy). The expected E^\pm energies for sample B are shown in the Fig.4(a), using a value of $\delta=0.03$ meV for the adjustable interaction parameter. To derive the unperturbed modes we have neglected the small Knight shift corrections assuming $E_{Mn}^S = g_{Mn}\mu_B B - 4D$ and E_e^S given by Eq.(1) with the Mn^{2+} polarization described by a Brillouin function and the relevant parameters obtained for this sample from low field transport measurements ($\Delta_E^{\max} = 1.65\text{meV}$, $T_0 = 0.18\text{K}$). Reasoning in terms of the mean field approach we would expect the 230GHz resonance to occur at a magnetic field just after the sup-

posed crossing point of the E_e^S and E_{Mn}^S energies. However, the effective resonating branch at 230GHz turns out to be the E^+ coupled mode. As emphasized in Fig.4, our simple model explains the actual resonance position and also accounts for the temperature dependence (with increasing temperature the crossing point for E_e^S and E_{Mn}^S excitations shifts towards lower fields). The correspondence with the experimental data good. The predicted resonance position is about 1 kG from the extrapolated value from the low field data and the temperature driven shift is of about 400 G in the range between 2 K to 4.2 K.

To further pursue the phenomenological interpretation of our experimental data, we refer to the theory of ferromagnetic resonance and consider the possibility that, when a spin polarization of Mn^{2+} and 2D electrons subsystems is induced by magnetic fields, each spin subsystem may constitute a collective (macroscopic) magnetic moment. Such collective modes are expected to efficiently interact via the transverse components, leading to mode repulsion with a characteristic interaction energy $(\Delta_E K_E)^{1/2}$ [10]. For sample B, we have determined $\Delta_E = 1.65\text{meV}$ from low field transport [11] and deduce that $K_E \lesssim 1.5\mu\text{eV}$, the equality occurring for the case where we have an ideal spin polarization of the 2DEG at $\nu = 3$. Therefore, in the upper limit $(\Delta_E K_E)^{1/2} = 0.05\text{meV}$ which is in fair agreement with the experimentally found interaction parameter $\delta = 0.03\text{meV}$. This agreement is even better for sample A with lower electron concentration, for which the 2DEG is very likely fully polarized at the (anti)crossing point ($B \simeq 6\text{T}$, $\nu = 0.7$). There, we expect $(\Delta_E K_E)^{1/2} = 0.03\text{meV}$ and measure $\delta \simeq 0.04\text{meV}$ (see Fig.1).

Summarizing, we have investigated a very diluted magnetic semiconductor system of Mn^{2+} ions coupled to a 2DEG in CdMnTe quantum well structures. The observed avoided crossing of the Mn^{2+} and the electron spin excitations is in agreement with recent theoretical predictions [10] and is a signature of the collective character of the spin excitations in DMS with free carriers.

We thank J. König and A.H. MacDonald for showing us their theoretical results prior to publication. Support from INTAS 99-01146, Polonium, EU-SPINOSA-IST-2001-33334., and PBZ-KBN-044/P03/2001 grants is acknowledged.

* Permanent address Institute for Microstructural Sciences, National Research Council, Ottawa, Canada K1A 0R6

- [1] T. Story et al., Phys. Rev. Lett. **56**, 777 (1986).
- [2] A. Haury et al., Phys. Rev. Lett. **79**, 511 (1997).
- [3] H. Ohno et al., Phys. Rev. Lett. **68**, 2664 (1992).
- [4] H. Ohno et al., Appl. Phys. Lett. **69**, 363 (1996).

- [5] T. Dietl et al., *Science* **287**, 1019 (2000).
- [6] M. Bercin and R. N. Bhatt, cond-mat/0204092.
- [7] J. König et al., *Phys. Rev. Lett.* **84**, 5628 (2000).
- [8] C. Kittel, *Introduction to Solid State Physics* (Wiley, New York, 1976).
- [9] C. Zener, *Phys. Rev.* **81**, 440 (1951).
- [10] J. König and A. H. MacDonald, submitted *Phys. Rev. Lett.* (2002).
- [11] F.J. Teran et al, *Phys. Rev. Lett* **88**, 186803 (2002).
- [12] A.A. Sirenko et al., *Phys. Rev. B* **56**, 2114 (1997).
- [13] M.F. Deigen et al., *Sov. Phys. - Solid State* **9**, 773 (1967).